Order-Disorder and Segregation Behavior at the $Cu_3Au(001)$ Surface

T. M. Buck and G. H. Wheatley
Bell Laboratories, Murray Hill, New Jersey 07974

and

L. Marchut[a]
University of Pennsylvania, Philadelphia, Pennsylvania 19104

(Received 7 December 1981; revised manuscript received 25 April 1983)

With use of low-energy Ne^+ scattering and low-energy electron diffraction both long-range order and Au segregation have been found at the $Cu_3Au(001)$ surface. The Au concentrations in the first and second layers are essentially constant at 0.5 and 0, respectively, for $T \leq 400\,^\circ C$, beyond which they approach each other. Calculations of shadowing for the ordered surface agree with experiment, e.g., for shadowing of Cu atoms in the second and third layers by Au atoms in the first layer.

PACS numbers: 68.20.+t, 64.60.Cn, 64.75.+g, 79.20.Nc

Cu_3Au is a classic ordering alloy, with negative enthalpy of mixing and a critical bulk ordering temperature $T_c = 390\,^\circ C$. The bulk ordering has been studied extensively.[1] One may ask if the ordered bulk arrangement [Fig. 1(a)], determined by x-ray diffraction, extends to the surface and, if so, which layer is on top, the 50-50 Au-Cu or pure Cu; if antiphase domains and/or steps result in a mixed surface; and if surface segregation of either element occurs. Low-energy electron-diffraction (LEED) studies[2] of the (001) surface showed long-range order which decreased continuously with increasing temperature, not abruptly at 390 °C as for bulk order. Another LEED study[3] found long-range order on the (001) and (111) surfaces but not the (011). The first-layer type (Au-Cu or Cu) on the (001) surfaces was not established in these studies nor was segregation reported, but Au enrichment was found by Auger electron spectroscopy (AES) on polycrystalline Au-Cu films and a single-crystal $Cu_3Au(111)$ surface[4a] and attributed to surface energy difference adjusted for atom size.[4b] A prediction that ordering and segregation would inhibit each other was made in a theoretical analysis.[5]

Since the ordering and segregation of interest occur in the first few atom layers, exceptional surface sensitivity is required for composition analysis, such as that of low-energy ion scattering (LEIS, or ion-scattering spectroscopy, ISS).[6,7] In this work we have used LEIS(TOF), the time-of-flight version of low-energy ion scattering,[8,9] which collects both the scattered neutrals and ions, thereby avoiding the neutralization questions which attend electrostatic analysis of noble-gas ions. The $Cu_3Au(001)$ target[10] was mounted on a button heater in a two-axis goniometer. The

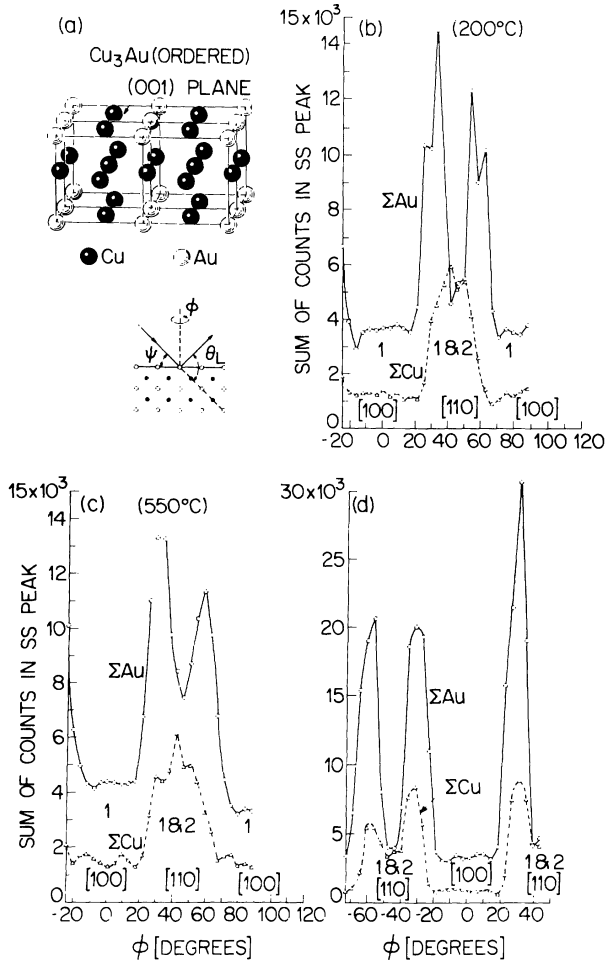

FIG. 1. (a) Upper: Ordered arrangement of Au and Cu in the bulk. Lower: Scattering geometry. (b)–(d) Single-scattering yield from Au and Cu as function of azimuthal angle φ. Incidence angle $\psi = 45°$. (b) 5-keV Ne on ordered surface; (c) 5-keV Ne on disordered surface; (d) 9.5-keV Ne on ordered surface. The crystal was remounted between scans (c) and (d), shifting the scan limits by about 50°.

UHV scattering chamber has a 95-cm flight leg and contains a LEED-Auger system and sputter gun.

With a pulsed Ne^+ beam of 5- or 9.5-keV energy, incident at $\psi = 45°$ or 35° from the surface plane and scattered through 90°, variations of azimuthal angle φ on the (001) surface permitted composition analysis of the first and second layers and identification of scattering from Au and Cu in the third layer. With the scattering plane parallel to a [100] azimuth and $\psi = 45°$ (⟨110⟩ axis in and out), single scattering events are restricted to the first layer; atoms in deeper layers are shadowed by the first-layer atoms. The well-defined single-scattering peaks for Cu and Au are summed[11] after subtracting a background due to double and multiple scattering (8%–20% for Au, 40%–60% for Cu, depending on temperature). The first-layer Au/Cu ratio is

$$N_{Au}/N_{Cu} = (Y_{Au}/Y_{Cu})(\sigma_{Cu}/\sigma_{Au})/d$$

in which N is the number of atoms exposed to the beam, Y is the scattered yield of Ne ions plus neutrals, σ is the differential scattering cross section derived from the Molière approximation to the Thomas-Fermi potential,[12] and d corrects for energy dependence of detector sensitivity. If no foreign atoms are present the atom fraction of Au in the first layer is then

$$X_1^{Au} = (N_{Au}/N_{Cu})/(1 + N_{Au}/N_{Cu}).$$

At 5 keV, $\sigma_{Au}/\sigma_{Cu} = 2.41$ and $d = 1.2$. The second-layer composition is determined from the scattering yield of both first and second layers measured along a [110] azimuth at $\psi = 35°$ incidence angle (⟨111⟩ axis in) (Au background 20%–30%, Cu 35%–60%). Single scattering is observed only from the first two layers. Scattering from second-layer atoms is enhanced by "wedge focusing"[13] in which the shadow cones of first-layer atoms concentrate ion flux on second-layer atoms. This is taken into account by the introduction of focusing factors which relate the scattering yields and compositions of the first and second layers as follows:

$$f_{Cu} = \left(\frac{Y_{1+2} - Y_1}{Y_1}\,\frac{X_1}{X_2}\right)^{Cu}. \qquad (1)$$

A similar relation holds for Au, and it can be shown that

$$X_2^{Au} = F\left[\frac{(Y_{1+2} - Y_1)^{Cu}}{(Y_{1+2} - Y_1)^{Au}}\,\frac{Y_1^{Au}}{Y_1^{Cu}}\,\frac{X_1^{Cu}}{X_1^{Au}} + F\right]^{-1}, \qquad (2)$$

in which $F = f_{Cu}/f_{Au}$, and other quantities are measured. We assume $F = 1$ without serious error, we believe, especially in the temperature region of disorder above 400 °C where X_2^{Au} first becomes significant.

Figures 1(b)–(d) show variations in single-scattering yield from Cu and Au [Σ_{SS}(Cu) and Σ_{SS}(Au)] as a function of azimuthal angle, at $\psi = 45°$, for three conditions. Scattering of 5-keV Ne from an ordered surface, annealed overnight at 200 °C but measured at room temperature, is shown in Fig. 1(b). The broad minima centered around the [100] azimuths represent first-layer scattering and the yield ratio $\Sigma(Au)/\Sigma(Cu) = 2.93$ corresponds to the composition $Au_{0.5}Cu_{0.5}$. [The low value of Σ(Au) at $\varphi = -15°$ was not reproduced in later measurements.] At the [110] azimuth, where both first and second layers are exposed, Σ(Cu) reaches a value 4.7 times the [100] value, while Σ(Au) is only 1.25 times the [100] value; the second layer is mainly Cu and Eq. (2) gives a second-layer composition of $Au_{0.06}Cu_{0.94}$. The layer compositions correspond closely to the arrangement of Fig. 1(a). A scan taken at 550 °C, well above T_c, is shown in Fig. 1(c). The increase in Σ(Au) at the [110] azimuth indicates enrichment of Au in the second layer. Compositions derived in this case are first layer $Au_{0.48}Cu_{0.52}$, second layer $Au_{0.20}Cu_{0.80}$. At this temperature (100) layers in the bulk must have the average bulk composition $Au_{0.25}Cu_{0.75}$ and the second layer has nearly reached it, but in the first layer surface segregation prevails.

The first- and second-layer compositions as functions of temperature are shown in Fig. 2. Annealing times before LEIS(TOF) analysis at temperature were 60–70 h at 25 °C, 20 h at 100 and 200 °C, 4 h at 300–450 °C, and 2–3 h at higher temperature. X_1^{Au} is constant at ~0.52 up to 400 °C but then decreases to 0.38 at 830 °C, presumably heading for 0.25. Competition between ordering and segregation must cause the change in slope at 400 °C. Similar behavior has been predicted for the (011) surface of $A_{0.5}B_{0.5}$ bcc ordering alloys.[14] Ordering dominates below T_c, but the relatively weak Au segregation tendency may aid in keeping X_1^{Au} at ~0.5 up to 400 °C even though LEED superlattice spots fade progressively at lower T,[2] evidently indicating only intraplanar disorder. Segregation also prevents a sharp drop to 0.25 at 400 °C. The entropy term in the free energy of segregation $\Delta F_S = \Delta H_S - T\Delta S_S$ should aid segregation below T_c but oppose it above, since segregation represents less order and more order, respectively, in the two

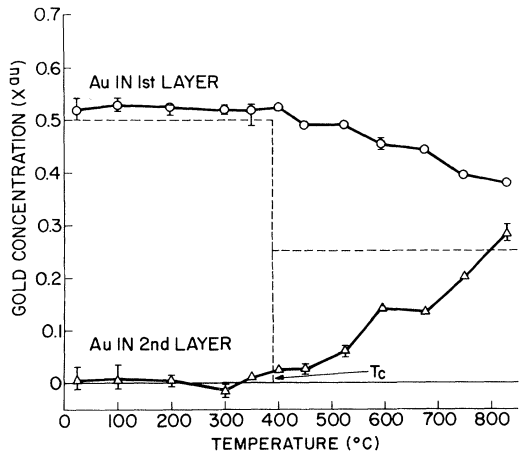

FIG. 2. Compositions of first and second layers of $Cu_3Au(001)$ as function of annealing temperature. Error bars and symbols without bars indicate the spread in three or more measurements on two or three spots. Dashed lines depict hypothetical abrupt transition.

cases. The fact that X_2^{Au} increases only gradually beyond 400 °C, as X_1^{Au} decreases, we attribute to the Au-Cu bonding preference. [The disagreement between $X_2^{Au} = 0.20$ at 550° from Fig. 1(c) and the value shown in Fig. 2, we ascribe to better statistics and longer annealing in the measurements of Fig. 2.] The Au segregation tendency must be responsible for the fact that the 50-50 Au-Cu layer was invariably on top after numerous sputter-cleaning and annealing sequences.

In addition to the layer compositions and LEED patterns as evidence of long-range order in the first and second layers, we find evidence of lattice-site ordering in the azimuthal scans. In Fig. 1(b) for 5-keV Ne^+ there are two notched peaks in Σ(Au) centered at 30° from the nearest [100] azimuths, but no corresponding maxima in Σ(Cu) which is peaked instead at the [110] azimuth. However, at 9.5 keV, Fig. 1(d), maxima do appear in the Σ(Cu) curve at $\varphi = 30°$ in phase with the Σ(Au) curve. With very little Au in the second layer, scattering from third-layer Au must be suspected at $\varphi = 30°$ and this possibility is supported by a higher degree of ion neutralization and by the shadow-cone analysis of Figs. 3(a)–3(d). The diagrams are based on a calculation[15] which determines the radius of the shadow cone[16] (envelope of trajectories of ions deflected by the screened Coulomb potential of a shadowing atom) in a plane normal to the beam direction and containing the target atom, and compares the radius with the distance in this plane from

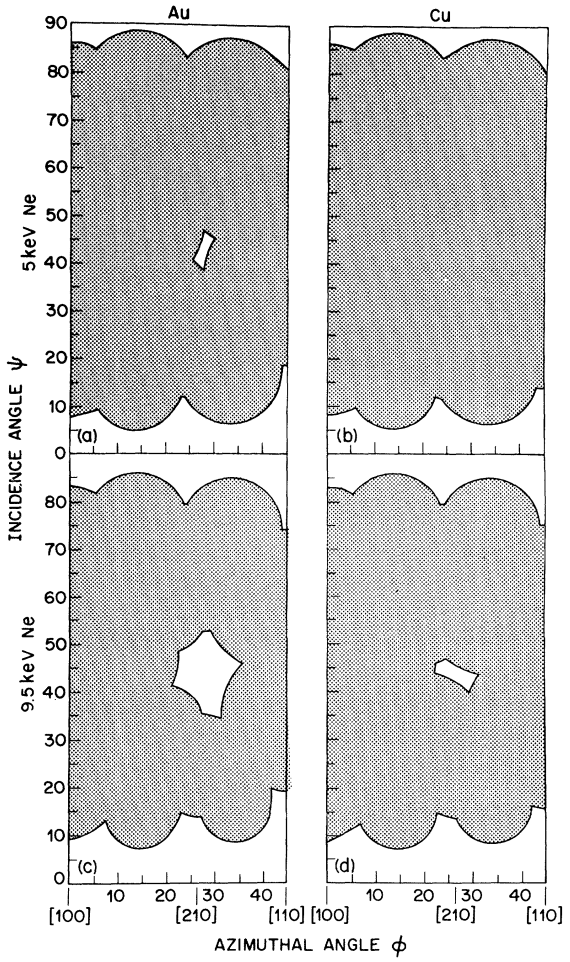

FIG. 3. Shaded areas map calculated combinations of ψ and φ for which single (but not multiple) scattering of Ne through 90°, by Cu or Au atoms in third layer, is prohibited by shadowing and/or blocking. Incident energy 5 keV in (a) and (b), 9.5 keV in (c) and (d).

the cone axis to the target atom. Blocking cones of atoms in or near the outgoing path are also taken into account. The analysis[15] is similar to that used[17] for scattering of Ne^+ ions from Cu-(110) in the use of an a/r^2 potential, but here the screening length was reduced by 20% and a more exact treatment used for the shadow-cone projection. Several facts are evident from Figs. 1 and 3: In the ordered condition Cu atoms in the third layer are shadowed at $\varphi = 30°$, $\psi = 45°$, and 5-keV energy, but Au atoms are not. This difference arises from the fact that at this orientation a third-layer Cu atom is shadowed by two gold atoms in the first layer (one row over), whereas third-layer Au atoms are shadowed by Cu atoms. The Au shadow cones are larger, with a radius of 1.4 Å vs 1.03 Å for Cu at a dis-

tance of 4.0 Å, and there is no "hole" in Fig. 3(b) for Cu at $\psi = 45°$, $\varphi = 30°$ but there is in 4(a) for Au. However, for 9.5-keV Ne^+ the shadow cones are smaller and Cu atoms in the third layer are exposed to the beam, producing a maximum in Σ(Cu) in phase with that in Σ(Au) at $\varphi = 30°$ [Fig. 1(d)] and a small opening centered at (27, 43) in Fig. 3(d). The Σ(Au) peaks in Fig. 1(b) indicate f_{Au}(third layer) = 2.3–3, not unreasonable,[11] but factors of 5–8 indicated in Fig. 1(d) are surprising; some fifth-layer scattering is suspected. Not only is the third-layer Cu shadowed from 5-keV Ne at $\varphi = 30°$ and 60° but so is half of the second-layer Cu, according to a second-layer shadow calculation not shown here, and the Σ(Cu) curve in Fig. 1(b) confirms this. This partial shadowing probably involves only the second-layer Cu in [100] rows beneath Au rows. Computer simulation of the scattering will be needed for more complete understanding of the scattering behavior[18] but the shadow-cone analysis is a useful first step.

This work was partially supported by the U. S. Office of Naval Research.

---

[a]Present address: Bell Laboratories, Murray Hill, N.J. 07974.

[1]R. Smoluchowski, in *Handbook of Physics*, edited by E. U. Condon and H. Odishow (McGraw-Hill, New York, 1967), pp. 8–97.

[2]V. S. Sundaram, R. S. Alben, and W. D. Robertson, Surf. Sci. 46, 653 (1974).

[3]H. C. Potter and J. M. Blakely, J. Vac. Sci. Technol. 12, 635 (1975).

[4a]J. M. McDavid and S. C. Fain, Jr., Surf. Sci. 52, 161 (1975); C. G. Shaw and S. C. Fain, Jr., in *Proceedings of the Seventh International Vacuum Congress and the Third International Conference on Solid Surfaces, Vienna, 1977*, edited by R. Dobrozemsky *et al.* (F. Berger and Söhne, Vienna, 1977), p. 2315.

[4b]A. R. Miedema, Z. Metallkd. 69, 455 (1978).

[5]J. L. Moran-Lopez and K. H. Bennemann, Phys. Rev. 15, 4769 (1977).

[6]D. P. Smith, J. Appl. Phys. 38, 340 (1967).

[7]H. H. Brongersma, M. J. Sparnaay, and T. M. Buck, Surf. Sci. 71, 657 (1978).

[8]Y. S. Chen, G. L. Miller, D. A. H. Robinson, G. H. Wheatley, and T. M. Buck, Surf. Sci. 62, 133 (1977).

[9]S. B. Luitjens, A. J. Algra, E. P. Th. M. Suurmeijer, and A. L. Boers, Appl. Phys. 21, 205 (1980).

[10]This Cu_3Au crystal was obtained from B. F. Addis, Department of Materials Science and Engineering, Cornell University, Ithaca, New York.

[11]T. M. Buck, G. H. Wheatley, and L. K. Verhey, Surf. Sci. 90, 635 (1979).

[12]The computer program for cross sections was written by Yu Su Chen of Bell Laboratories and based on analysis of M. T. Robinson and I. M. Torrens, Phys. Rev. B 9, 5008 (1974).

[13]H. H. W. Feijen, L. K. Verhey, E. P. Th. M. Suurmeijer, and A. L. Boers, in *Atomic Collisions in Solids*, edited by S. Datz *et al.* (Plenum, New York, 1975), Vol. 2, p. 573.

[14]J. L. Moran-Lopez and L. M. Falicov, Phys. Rev. B 18, 2542 (1978).

[15]L. Marchut, Ph.D. thesis, Department of Materials Science and Engineering, University of Pennsylvania (unpublished).

[16]W. Turkenburg, W. Soszka, F. W. Saris, H. H. Kersten, and B. G. Colenbrander, Nucl. Instrum. Methods 132, 587 (1976).

[17]R. P. N. Bronckers and A. G. J. deWit, Surf. Sci. 104, 384 (1981).

[18]D. P. Jackson, T. M. Buck, and G. H. Wheatley, to be published.